Short communication

Dehydrogenation and hydrogenation characteristics of MgH$_2$ with transition metal fluorides

Seon-Ah Jin [a,b], Jae-Hyeok Shim [a], Young Whan Cho [a,*], Kyung-Woo Yi [b]

[a] *Materials Science and Technology Research Division, Korea Institute of Science and Technology, Seoul 136-791, Republic of Korea*
[b] *Department of Materials Science and Engineering, Seoul National University, Seoul 151-742, Republic of Korea*

Abstract

The effect of transition metal fluorides on the dehydrogenation and hydrogenation of MgH$_2$ has been investigated. Many of the fluorides show a considerable catalytic effect on both the dehydrogenation temperature and hydrogenation kinetics of MgH$_2$. Among them, NbF$_5$ and TiF$_3$ most significantly enhance the hydrogenation kinetics of MgH$_2$. It is suggested that hydride phases formed by the reaction between MgH$_2$ and these transition metal fluorides during milling and/or hydrogenation play a key role in improving the hydrogenation kinetics of MgH$_2$.
© 2007 Elsevier B.V. All rights reserved.

Keywords: Hydrogen storage; Magnesium hydride; Transition metal fluoride; Ball milling; Catalysis; Reaction kinetics

1. Introduction

Magnesium hydride (MgH$_2$) is a promising material for hydrogen storage applications as it has high gravimetric (7.6 wt.%) and volumetric (110 kg m^{-3}) densities. Moreover, its reversibility and cycle performance are quite good compared with other group I and II binary and complex hydrides. Nevertheless, a high desorption temperature and slow sorption kinetics are the main problems to be solved before MgH$_2$ can be seriously considered as a practical material for high-capacity, solid-state, hydrogen storage systems.

Although the high desorption temperature still remains to be solved, the sorption kinetics of MgH$_2$ have been dramatically improved by ball-milling MgH$_2$ with some transition metals and their oxides [1–6]. It has also been found that some transition metal halides, such as CrCl$_3$, FeF$_3$, NiF$_2$, TiF$_3$ NbCl$_5$ and NbF$_5$, also show very good catalytic property [7–14]. On the other hand, the addition of group I and II halides show an insignificant effect on the dehydrogenation kinetics of MgH$_2$ [7]. Nevertheless, it is still not clear how these chemically different additives promote the dehydrogenation and hydrogenation reactions of MgH$_2$.

In this work, nine different transition metal fluorides are tested to investigate systematically their catalytic effect on the dehydrogenation and hydrogenation characteristics of as-received commercial MgH$_2$ powder. Explanations why certain transition metal fluorides show a better catalytic effect than others are given in terms of the change in chemistry of the halide additives after milling or thermal decomposition.

2. Experimental

A high-energy ball-milling technique was adopted to disperse transition metal fluorides homogeneously and induce mechano-chemical reactions between these fluorides and MgH$_2$, simultaneously. One gram of MgH$_2$ (98%) containing 1–10 mol% of each fluoride was charged with ten 7.9 mm diameter Cr-steel balls into a 70-ml hardened-steel vial and then milled for 15 min by means of a SPEX-8000 vibratory mill. All handling of the samples, except the milling, were done in a glove-box under argon atmosphere. Both the oxygen and water vapour levels inside the glove-box were kept below 1 ppm. The thermal decomposition behaviour of the milled samples was evaluated with a Netzsch 204 F1 Phoenix differential scanning calorimeter (DSC) under high-purity argon (99.9999%). The hydrogenation kinetics were measured with a Netzsch 204 HP Phoenix high-pressure DSC. During the hydrogenation step, the

---

dynamic pressure and flow rate of hydrogen (99.9999%) were maintained at 10 bar and 10 ml min^{-1}, respectively. The actual hydrogen contents of the hydrogenated samples, as well as the as-milled samples, were separately determined with a Netzsch 209 F1 Thermogravimeter (TG) coupled to a Netzsch 403C mass spectrometer. The phase compositions of the as-milled samples and those after thermal decomposition at 300 °C under vacuum were obtained with a Bruker D8 Advance X-ray diffractometer (XRD) with Cu Kα radiation. A special air-tight sample holder was used to prevent any possible reactions between the sample and air during XRD measurements.

3. Results and discussion

The DSC curves of MgH$_2$ with 1 mol% of transition metal fluorides are shown in Fig. 1. Except for Cu and Y fluorides, all the other fluorides examined in the present study significantly decrease the decomposition temperature of MgH$_2$. Among them, Ni, Ti, V, and Nb fluorides are more effective than Fe, Zr, and Cr fluorides. CuF$_2$ shows very small catalytic effect and there is virtually no catalytic effect with YF$_3$. It is noted that the decomposition temperature range of NbF$_5$ is wider than that of other transition metal fluorides.

There may be several reasons why Cu and Y halides have no discernable catalytic effect on the thermal decomposition of MgH$_2$. One is that they form stable intermetallic compounds with Mg and these may be inactive. In fact, it has been reported [3] that the catalytic effect of CuO on the dehydrogenation of MgH$_2$ is much less than that of other transition metal oxides, although it has rather good catalytic effect on the hydrogenation reaction. Y has only one valence state (+3), while other transition metals tested in the present study have multi-valency. This may explain why YF$_3$, Sc$_2$O$_3$ [3], and CeF$_3$ (see Fig. 1) do not have a significant catalytic effect. Incidentally, Sc and Ce also form stable intermetallic compounds with Mg. Of course, Ni also forms stable intermetallic compounds with Mg but there is a stable ternary hydride Mg$_2$NiH$_4$ and its catalytic effect on the dehydrogenation kinetics of MgH$_2$ is already known [15].
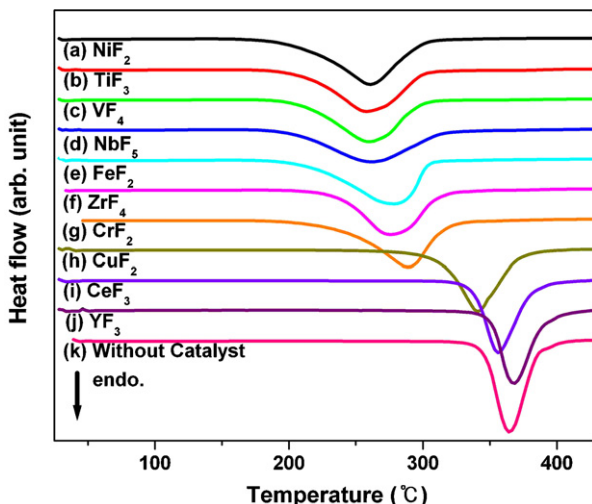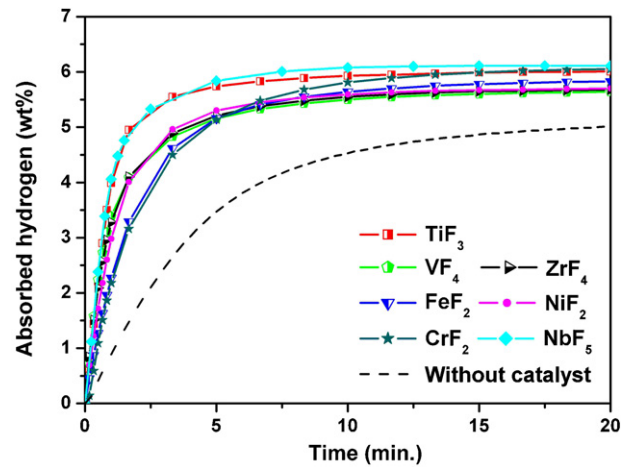

Fig. 2. Hydrogenation kinetics of MgH$_2$ at 573 K under 10 bar of hydrogen with 1 mol% transition metal fluorides.

The effect of transition metal fluorides on the hydrogenation kinetics of MgH$_2$ at 300 °C under 10 bar of hydrogen is presented in Fig. 2. The Nb and Ti fluorides show the fastest kinetics, while V, Zr, and Ni give similar, slower kinetics. The Fe and Cr fluorides report the slowest kinetics. These finding are in general agreement with those of DSC, i.e., the trend of the catalytic effect of these transition metal fluorides on both the dehydrogenation and hydrogenation reactions is similar. It is also interesting to note that NiF$_2$ does not show as fast kinetics as expected from the DSC study. On the other hand, NbF$_5$ gives hydrogenation kinetics much faster than expected. One of the reasons why NbF$_5$ has this significant catalytic effect is its low melting temperature (80 °C) and therefore the mechano-chemical reaction between MgH$_2$ and NbF$_5$ during ball-milling might have produced much finer and more homogeneously dispersed metal or metal hydride particles in MgH$_2$. It should be mentioned, however, that the melting point of TiF$_3$ is quite high (>1200 °C) but it still has as good catalytic effect as NbF$_5$. More details on the catalytic effect of NbF$_5$ are described elsewhere [14].

The XRD patterns of MgH$_2$ with 1 mol% of TiF$_3$ are shown in Fig. 3(a and b). In the as-milled state, β-MgH$_2$ and some
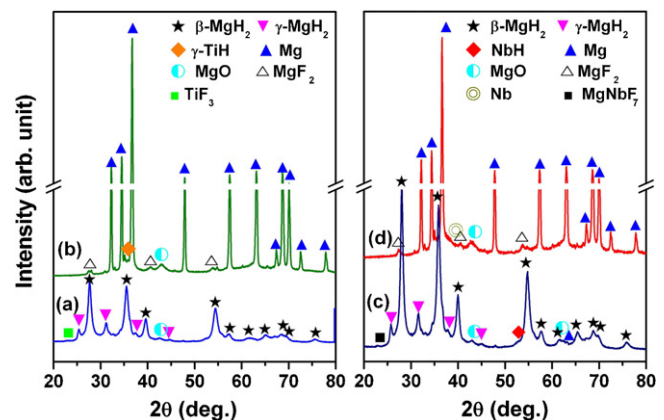

Fig. 1. DSC curves of MgH$_2$ with 1 mol% transition metal fluorides.

Fig. 3. XRD patterns of MgH$_2$ with: (a) 1 mol% TiF$_3$, as-milled; (b) 1 mol% TiF$_3$, after decomposition; (c) 1 mol% NbF$_5$, as-milled; (d) 1 mol% NbF$_5$, after decomposition.

γ-MgH$_2$ induced by high-energy ball-milling are observed, as well as Mg, MgO and a trace of unreacted TiF$_3$ (Fig. 3(a)). The presence of MgF$_2$ and Ti or Ti hydrides including TiH$_2$, if any, could not be clearly detected due to their small volume fraction and low electron density (for MgF$_2$) as well as the very broad peaks of milled MgH$_2$. Mg, MgF$_2$ and γ-TiH [16] are detected in the sample after dehydrogenation at 350 °C under vacuum (<10^{-5} bar), as shown in Fig. 3(b). This agrees in general with the result of the previous report of Ma et al. [12] who observed 'TiH$_2$' after dehydrogenation at 300 °C under 0.1 bar of hydrogen. The presence of γ-TiH instead of the equilibrium δ-TiH$_2$ phase is not unexpected as δ-TiH$_2$ decomposes, according to thermodynamic calculation, even at 350 °C if the partial pressure of hydrogen is maintained below 10^{-5} bar, which is the case in the present study. It is believed that TiH$_2$ forms by the following displacement reaction during milling process:

$$3MgH_2 + 2TiF_3 \rightarrow 3MgF_2 + 2TiH_2 + H_2 \qquad (1)$$
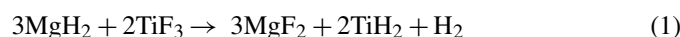
but subsequently decomposes partly into TiH + 0.5H$_2$ during heating under a dynamic vacuum. The sample with 1 mol% of ZrF$_4$ shows a similar result, which is not included here.

The sample with 1 mol% of NbF$_5$ also exhibits similar behaviour (Fig. 3(c)) to that with 1 mol% of TiF$_3$. In the dehydrogenated sample (Fig. 3(d)), Nb and NbH$_x$ (x < 1) are observed together with Mg, MgF$_2$ and MgO. Unlike Ti, Nb hydrides are not stable at elevated temperatures unless the hydrogen partial pressure is kept above 1 bar [17], and this appears to be the reason why Nb and NbH$_x$ exist in the sample decomposed under vacuum. It is noted that the width of the diffraction peak from Nb (or more probably a Nb–H solid solution) is quite broad. This indicates that the size of the crystallites is extremely small and this might have contributed to enhancing the catalytic effect of NbF$_5$ significantly. More details about the microstructure of and the distribution of Nb–H phases in MgH$_2$ with 1 mol% of NbF$_5$ are reported elsewhere [14]. On the other hand, neither vanadium hydride nor a V–H solid solution is observed in the as-milled sample with 1 mol% of VF$_4$. This is expected as these two materials are not stable, even at room temperature, unless the hydrogen partial pressure is very high.

Fe does not form any solid solutions or intermetallic compounds with Mg but it forms a very stable ternary hydride Mg$_2$FeH$_6$. It is, therefore, expected that Mg$_2$FeH$_6$ will develop during milling via the following reaction:

$$3MgH_2 + FeF_2 \rightarrow Mg_2FeH_6 + MgF_2 \qquad (2)$$
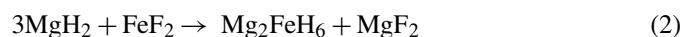
The XRD pattern of the sample with 10 mol% FeF$_2$ after milling for 70 min clearly shows the existence of Mg$_2$FeH$_6$ as well as free Fe (Fig. 4(a)). Moreover, a prolonged milling time increases Mg$_2$FeH$_6$ but decreases Fe, which clearly indicates that the above reaction is actually a two step process as follows:

$$MgH_2 + FeF_2 \rightarrow MgF_2 + Fe + H_2 \qquad (3)$$

$$2MgH_2 + Fe + H_2 \rightarrow Mg_2FeH_6 \qquad (4)$$
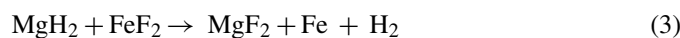
This result is somewhat different from those of others [8–10] who did observe elemental Fe, but not Mg$_2$FeH$_6$, in their as-milled samples. It is believed the milling energy of the vibrating
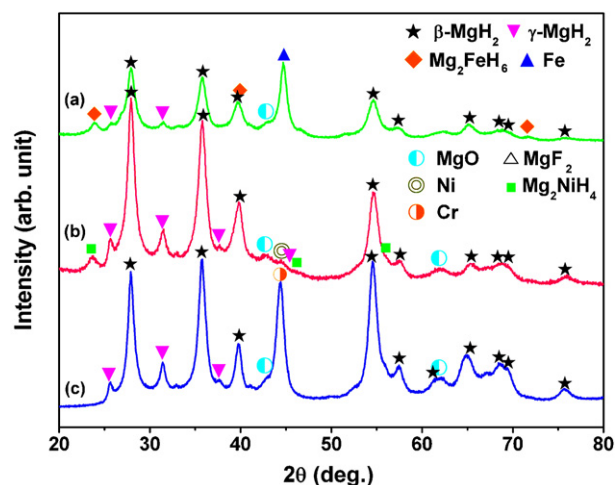

Fig. 4. XRD patterns of MgH$_2$ with: (a) 10 mol% FeF$_2$, as-milled for 70 min; (b) 5 mol% NiF$_2$, as-milled for 70 min; (c) 5 mol% CrF$_2$, as-milled for 4 h.

mill used by them is much lower than the SPEX-8000 mill employed in the present study.

Ni also forms a stable ternary hydride Mg$_2$NiH$_4$ (Fig. 4(b)), but Cr does not react with Mg nor form any stable binary or ternary hydrides. The XRD pattern of MgH$_2$ with 5 mol% of CrF$_2$ (Fig. 4(c)) clearly shows the existence of free Cr. It has also been reported that Cr$_2$O$_3$ exerts a beneficial catalytic effect on the sorption kinetics of MgH$_2$ [3].

According to the thermodynamic stabilities of the nine different transition metal fluorides tested in the present study, all of them are expected to react with MgH$_2$ to produce much more stable MgF$_2$ and either free metals or hydrides (or even intermetallic compounds), if the activation barrier of these solid–solid reactions can be effectively removed by mechano-chemical activation during high-energy ball-milling, or by thermal activation during the dehydrogenation process. In order to check the validity of this presumption, the thermodynamic equilibrium of MgH$_2$ with different transition metal fluorides has been calculated by Thermo-Calc [18] and the results are summarized in Table 1. The calculation could not be carried out for NiF$_2$, FeF$_2$ and YF$_3$, as the thermodynamic data of MgNiH$_4$, Mg$_2$FeH$_6$ and Mg–Y intermetallic phases are not available. According to the thermodynamic calculation, the transition metal fluorides tested in the present study are categorized into three groups: (i) CrF$_2$ is reduced to metal Cr; (ii) Ti, Zr, V and Nb fluorides form binary hydrides, although vanadium

Table 1
Calculated equilibrium transition metal phase in MgH$_2$-transition metal fluoride systems

Additives	Equilibrium phase
TiF$_3$	TiH$_2$
VF$_4$	V$_3$H$_2$
NbF$_5$	NbH
ZrF$_4$	ZrH$_2$
CrF$_2$	Cr
CuF$_2$	Cu$_2$Mg
CeF$_3$	CeH$_2$

hydride may not be stable at elevated temperatures under 1 bar of H_2; (iii) Cu forms an intermetallic compound with Mg. The results of XRD analysis on as-milled samples, some of which are given in Figs. 3 and 4, confirm these thermodynamic predictions.

4. Conclusions

In this paper, transition metal fluorides that readily react with MgH_2 to form hydrides or metal–hydrogen solid solutions tend to exert a significant catalytic effect on the hydrogenation kinetics of MgH_2. On the other hand, those elements which (a) form stable intermetallic phases with Mg but not any hydrides or (b) have single valency appear to have little or virtually no catalytic effect. Thus, it appears that the actual phases that act as an effective catalyst are not fluorides, but hydrides, although a certain auxiliary role of MgF_2 by-product, which may have preferably segregated on the surface, and grain boundaries of MgH_2 cannot be discounted.

Acknowledgement

References

[1] A. Zaluska, L. Zaluski, J.O. Strom-Olson, J. Alloys Compd. 289 (1999) 197–206.

[2] G. Liang, J. Hout, S. Boily, A. van Neste, R. Schulz, J. Alloys Compd. 291 (1999) 295–299.

[3] W. Oelerich, T. Klassen, R. Bormann, J. Alloys Compd. 315 (2001) 237–242.

[4] G. Barkhordarian, T. Klassen, R. Bormann, Scr. Mater. 49 (2003) 213–217.

[5] O. Friedrichs, T. Klassen, J.C. Sanchez-Lopez, R. Bormann, A. Fernandez, Scr. Mater. 54 (2006) 1293–1297.

[6] O. Friedrichs, F. Aguey-Zinsou, J.R. Fernandez, J.C. Sanchez-Lopez, A. Justo, T. Klassen, R. Bormann, A. Fernandez, Acta Mater. 54 (2006) 105–110.

[7] E. Ivanov, I. Konstanchuk, B. Bokhonov, V. Boldyre, J. Alloys Compd. 359 (2003) 320–325.

[8] J.F.R. de Castro, A.R. Yavari, A. LeMoulec, T.T. Ishikawa, W.J. Botta, J. Alloys Compd. 389 (2005) 270–274.

[9] A.R. Yavari, A. LeMoulec, J.F.R. de Castro, S. Deledda, O. Friedrichs, W.J. Botta, G. Vaughan, T. Klassen, A. Fernandez, A. Kvick, Scr. Mater. 52 (2005) 719–724.

[10] S. Deledda, A. Borissova, C. Poinsignon, W.J. Botta, M. Dornheim, T. Klassen, J. Alloys Compd. 404–406 (2005) 409–412.

[11] V.V. Bhat, A. Rougier, L. Aymard, X. Darok, G. Nazri, J.M. Tarascon, J. Power Sources 159 (2006) 107–110.

[12] L.-P. Ma, P. Wang, H.-M. Cheng, J. Alloys Compd., J. Alloys Compd. 432 (2007) 1–4.

[13] Y. Luo, P. Wang, L.-P. Ma, H.-M. Cheng, J. Alloys Compd., in press.

[14] S.-A. Jin, J.-P. Ahn, J.-H. Shim, Y.W. Cho, K.-W. Yi, Acta Mater., in press.

[15] G. Liang, J. Huot, S. Boily, A. Van Neste, R. Schultz, J. Alloys Compd. 292 (1999) 247–252.

[16] H. Numakura, M. Koiwa, H. Asano, F. Izumi, Acta Metall. 36 (1988) 2267–2273.

[17] J.F. Smith, Bull. Alloy Phase Diagrams 4 (1983) 39–46.

[18] http://www.thermocalc.se.